Design and Implementation of a Reaction Wheel System for CubeSats

N Sai Krishna
Manipal Institute of Technology
Manipal, Karnataka, India
+91-9008508613
nsai500@gmail.com

Sushmita Gosavi
Manipal Institute of Technology
Manipal, Karnataka, India
+91-9765195154
sushmitagosavi03@gmail.com

Shivika Singh
Manipal Institute of Technology
Manipal, Karnataka, India
+91-7899043081
shivikasingh275@gmail.com

Naman Saxena
Manipal Institute of Technology
Manipal, Karnataka, India
+91 9916886109
naman.saxena@outlook.com

Anirudh Kailaje
Manipal Institute of Technology
Manipal, Karnataka, India
+91 9481421254
anirudhkailaje@gmail.com

Vishwanath Datla
Manipal Institute of Technology
Manipal, Karnataka, India
+91 9632095522
viswanath.datla7@gmail.com

Paras Shah
Manipal Institute of Technology
Manipal, Karnataka, India
+91 7676445153
paras423@gmail.com

Abstract—**This paper describes the dynamics and control of a reaction wheel system for three axis control of a nano-satellite. The dynamics equations governing the reaction wheel system, the controller-reaction wheel interface and the motor control mechanism have been elaborated. The Controller-Reaction wheel interface which includes speed control of the motor of the reaction wheel system from the obtained torques has been described. Due to the presence of continuous disturbance torques in space the reaction wheels will saturate after a certain period, the momentum must be unloaded from the reaction wheels to use them again for attitude control. The results of a momentum dumping strategy using three magnetorquers have been discussed. The speed control system for the motor and the momentum dumping strategy have been tested using a SIL(Software-In-the-Loop) system and all the relevant results have been shown. The BLDC motor used requires a three phase supply. Since the on-board battery provides a DC voltage, power electronic circuits are used to convert this DC to a 3 phase AC using SVPWM method. SVPWM is used to reduce any possible vibrations in the motor due to supply harmonics. The rotor position and speed is determined by both hall effect sensors and the back emf measurements. Since the motor is a slow responding device with a large mechanical time constant, a PID controller is used to speed up any transitions in the rotor speed. The design of this controller has been discussed in detail.**

TABLE OF CONTENTS

978-1-5386-2014-4/18/$31.00 ©2018 IEEE

1. INTRODUCTION

Reaction wheels have become the most common actuators in CubeSats as they can achieve a high pointing accuracy. They apply torque on the system by changing the rotational speeds of the flywheels. Reaction wheels build up momentum over time which causes the motors to saturate at their maximum rotational speed. Magnetorquers are usually supplied alongside reaction wheels to dump this accumulated angular momentum by making use of the Earth's magnetic field. Different configurations of the reaction wheel system can be implemented.

This paper presents a system with a combination of three reaction wheels and three Magnetorquers. This paper covers the dynamics of the reaction wheel system, the electrical and mechanical design of the reaction wheel system for a 2U CubeSat, the control algorithm used for the satellite attitude control and the reaction wheel control along with the supporting results for the verification of the proposed system. The results are obtained using a 'Software-In-the-Loop' test bed which simulates the entire satellite configuration.

The electronic configuration of the reaction wheel system uses a BLDC (Brushless DC) motor as the primary driver for the reaction wheel and a PID controller used to drive the motor.

The mechanical design of the Reaction wheel - Magnetorquer system covers the structural analysis of the combination to ensure its survivability from the vibrations received during the launch phase of the satellite.

2. REACTION WHEEL DYNAMICS

Reaction wheels work on the principle of Law of Conservation of Angular Momentum. The angular momentum of a spinning satellite is transferred to the reaction wheels by rotating them thus decreasing the angular rate of the satellite. The dynamics equation of motion of a rigid spacecraft is given by Euler's Equations [1] as

$$\frac{dL}{dt} = T_{disturbance} + T_{control} - \omega_{bi} \times L \qquad (1)$$

where, L is the total angular momentum of the satellite,
$T_{disturbance}$ is the net disturbance torque acting on the satellite,

$T_{control}$ is the control torque acting on the satellite due to the magnetorquers and
ω_{bi} is the angular velocity of the satellite in body frame with respect to the inertial frame.

Here, L can be written as

$$L = I\omega_{bi} + L_{rw} \tag{2}$$

where, I is the principal moment of inertia matrix of the satellite and
L_{rw} is the angular momentum of reaction wheels.

Eq (1) can be written as follows

$$\frac{d}{dt}\big(I\omega_{bi}+L_{rw}\big) = T_{disturbance}+T_{control}-\omega_{bi}\times\big(I\omega_{bi}+L_{rw}\big) \tag{3}$$

$$\dot{\omega_{bi}} = I^{-1}\Big(T_{disturbance}+T_{control}-\dot{L_{rw}}-\omega_{bi}\times\big(I\omega_{bi}+L_{rw}\big)\Big) \tag{4}$$

where, $\dot{L_{rw}}$ indicates the rate of change of angular momentum of reaction wheels which is equal to the torque produced from the reaction wheels and $\dot{\omega_{bi}}$ is the rate of change of angular velocity of the satellite

This equation can be used to find the effect of torque applied on the satellite in terms of angular velocity of the satellite, which is used to simulate the orientation of the satellite in the next instance.

3. Attitude Control Flow

The satellite has two modes of control namely detumbling mode and pointing mode. In detumbling mode the angular velocity of the satellite is brought below 5 deg/sec. To decide on the mode of control, the value from gyroscope is used. If the angular rate of the satellite is below 5 deg/sec then the pointing mode is activated. Due to power constraints, a B-dot controller with three magnetorquers has been used for detumbling. In the pointing mode, three reaction wheels have been used for three axis pointing and to reduce the angular rates of the satellite even further. Due to the problem of saturation of speed of motor, magnetorquers have been used for dumping the excess momentum of the reaction wheels.
Figure 1 shows the in orbit flow of the attitude control of the satellite.
B-dot is a simple controller which requires only magnetorquers for actuation. The control torques from the B-dot controller are such that it decreases the rate of change of magnetic field measured. The magnetic moment from the B-dot controller [2] is given by

$$m = -k\frac{dB}{dt} \tag{5}$$

where, m is the magnetic moment of the magnetorquer,
k is a positive constant and
B is the Earth's magnetic field measured by the magnetometer.
The torque applied on the satellite will be as follows

$$T_{control} = m \times B \tag{6}$$

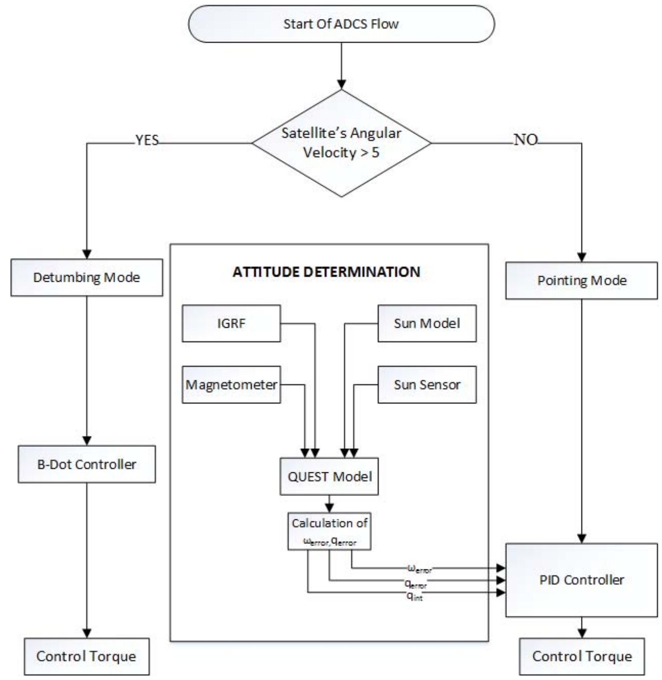

Figure 1. In Orbit Flow for Attitude Control

where, $T_{control}$ is the torque obtained by the magnetorquer.

In pointing mode, a Proportional-Integral-Derivative (PID) controller has been used. The inputs for the PID controller are q_{error}, integral of q_{error} (q_{int}) and ω_{error}. The q_{error} represents the rotation for achieving the desired attitude. It is obtained from the QUaternion ESTimator (QUEST) module which takes the ideal sun vector, ideal magnetic field vector, calculated sun vector from the measured sun sensor values and magnetic field vector from the magnetometer as the inputs.
The equation of the PID controller [3] can be given as

$$T_{control} = K_p.q_{error} + K_d.\omega_{error} + K_i.q_{int} \tag{7}$$

where, K_p,K_i and K_d are the proportional,integral and derivative gains respectively.
The values of these gains have been tuned according to the system to provide an optimal control torque. The control torque calculated is then applied by the reaction wheels. As the orientation changes by the application of torque, the sensors measure the new values, the error in orientation is calculated again and is fed into the controller. This process is repeated continuously to achieve the desired stability and attitude.

Determination of Reaction Wheel Speed

The torque which is obtained from the PID Controller needs to be applied on the satellite using the three reaction wheels. The following equation is used to determine the wheel speed that needs to be achieved for the required torque to be applied on the satellite.

$$T_{rw} = \dot{L_{rw}} \tag{8}$$

where, T_{rw} is the torque produced from the reaction wheels.

$$\dot{L_{rw}} = \frac{d}{dt}\big(I_{rw}\omega_{rw}\big) \tag{9}$$

where I_{rw} is the moment of inertia of the flywheel about its axis of rotation

ω_{rw} is the angular velocity of the flywheel

As the flywheel rotates in one direction producing a torque, an equal and opposite torque is produced on the satellite. So if the required torque from controller is T_c,an opposite torque needs to be produced by the flywheel.

$$T_{rw} = -T_c \tag{10}$$

$$\frac{d}{dt}\left(I_{rw}\omega_{rw}\right) = -T_c \tag{11}$$

$$\frac{I_{rw}\left(\omega_{new} - \omega_{previous}\right)}{steptime} = -T_c \tag{12}$$

where ω_{new} is the angular velocity of the flywheel that needs to be achieved for producing the required torque.
$\omega_{previous}$ is the previous angular velocity of the flywheel

Using the equation 12, the new wheel speed is calculated and after the new wheel speed is achieved in a particular step time, the required torque is produced about that axis.

4. Momentum Dumping for Reaction Wheels

The disturbance torques acting on the satellite will increase the angular momentum of the reaction wheels overtime which causes speeding of reaction wheels. Table 1 gives an understanding of the average value of disturbance torques for a CubeSat in the low Earth orbit.

Table 1. Disturbance Torques

Name	Magnitude (N-m)
Solar Radiation Pressure	4.487×10^{-10}
Aerodynamic Drag Torque	4.723×10^{-9}
Gravity Gradient Torque	7.98×10^{-10}

At a certain point the rotation speed of the motors saturate and there is a need to remove the accumulated angular momentum from the reaction wheels. This can be achieved using external torques from the magnetorquers. To maintain continuous attitude control, a continuous momentum dumping strategy[4] has been used.

$$m_{torquer} = \frac{-gain}{||B^2||}\left(B \times \Delta H_w\right) \tag{13}$$

where, $m_{torquer}$ is the magnetic moment of the magnetorquer required for momentum dumping of reaction wheels
B is the magnetic field in the body frame of the satellite
ΔH_w is the difference between the current angular momentum of the wheel and the ideal angular momentum of the wheel
For the simulations, the ideal angular momentum of the wheels is taken to be zero.
The torque from the magnetorquer ($T_{torquer}$) can be calculated by the following equation

$$T_{torquer} = m_{torquer} \times B \tag{14}$$

Since net torque of T_c should be applied on the satellite, it is allocated such that part of it is applied by the magnetorquer and the remaining torque is applied by the reaction wheels. The torque that needs to be produced by the reaction wheel is calculated from the following equation

$$T_{rw} = -\left(T_c - T_{torquer}\right) \tag{15}$$

Equation 12 is modified as follows

$$\frac{I_{rw}\left(\omega_{new} - \omega_{previous}\right)}{steptime} = -\left(T_c - T_{torquer}\right) \tag{16}$$

5. Simulation Results and Analysis

The control laws and the momentum dumping strategy are validated by performing a Software-in-the-loop(SIL) testing. The principal moment of inertia matrix of the satellite(in kg-m^2) is taken to be

$$I = \begin{bmatrix} 0.0115 & 0 & 0 \\ 0 & 0.0116 & 0 \\ 0 & 0 & 0.00446 \end{bmatrix} \tag{17}$$

The initial angular velocity of the satellite is taken to be [50 50 50]°/sec about all the three axis. The B-dot controller is run for the first 14000 seconds and then the PID controller is run if the angular rates are below 5 deg/sec about all the three axes. Based on these conditions, the results of q_{error}, angular rates of satellite and speed of the reaction wheels in RPM(Revolutions Per Minute) are shown for a period of 40000 seconds.

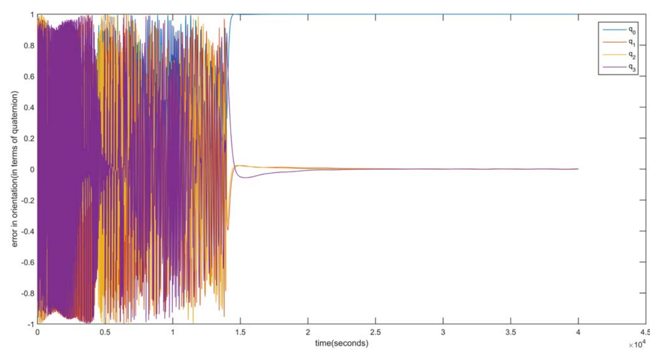

Figure 2. Error in Satellite's Orientation (in quaternion)

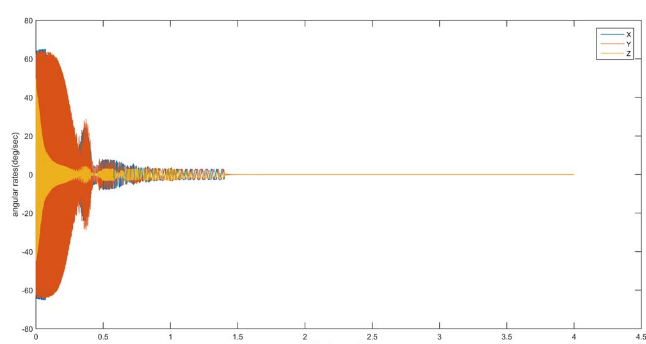

Figure 3. Angular Rates of satellite (in deg/sec)

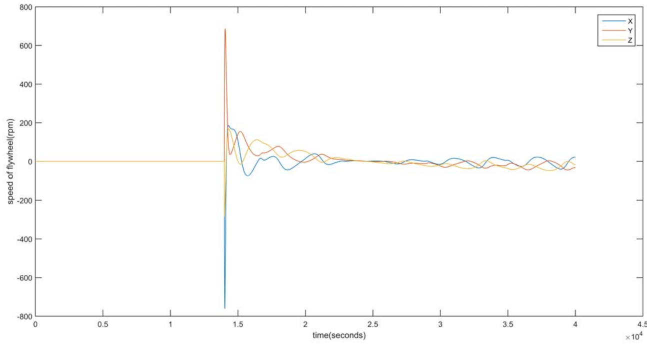

Figure 4. **Speed of Flywheel**

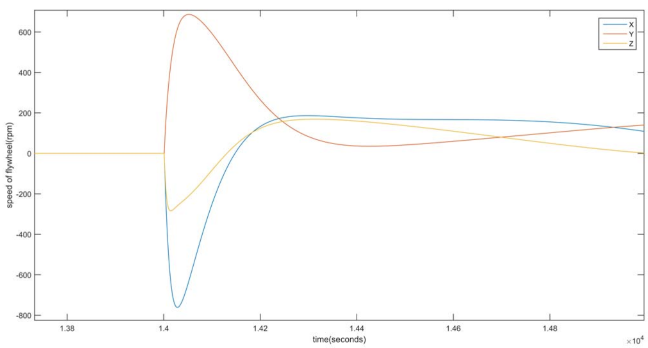

Figure 5. **Closer view of Flywheel Speed around 14000 seconds**

From figure 2, it can be observed that after the PID controller is started (after 14000 seconds and when angular rates are less than 5 deg/sec), the error in orientation is decreased and after a particular amount of time, the desired orientation is achieved (q_{error} has a value close to [1 0 0 0]). In figure 3, it can be observed that when the B-dot controller was run for 14000 seconds initially, the angular rates are brought down to around 5 deg/sec. In figure 4, a plot of the speed of the flywheel (in revolutions per minute) for 40000 seconds has been shown. Figure 5 shows a closer view of the speed of flywheel around 14000 seconds. The wheel speed rises initially according to required control torque. The continuous momentum dumping controller tries to bring the speed of the flywheel to zero. After a particular amount of time, we can observe that the desired orientation has been achieved and the required control torque also decreases. The dumping controller will allocate part of the control torque to the magnetorquers which will indirectly have an effect on the flywheel speed by bringing it down.

6. PID Control for Motor

Motor driver and PID controller

The motor driver uses the hall effect sensor signals to control the motor's speed. A PWM (Pulse Width Modulation) signal is used as input to the motor and the steady state motor speed is determined by the duty cycle of the PWM signal.
Speed control of a BLDC motor is easier compared to induction motors. PID controller is used primarily to reduce the rise time of the motor. The transfer function for a BLDC motor [5] is

$$G(s) = \frac{\frac{1}{K_e}}{\tau_m.\tau_e.s^2 + \tau_m.s + 1} \tag{18}$$

where, τ_{m} is the mechanical time constant,
τ_{e} is the electrical time constant and
K_{e} is the back emf constant.
In discrete time response, the equation translates to

$$G(z) = \frac{0.7946.z + 0.001855}{z^2 - 0.993.z} \tag{19}$$

The step response of this equation without the PID controller has a rise time (time taken to reach 90% of maximum value) of 20ms. It is converted from continuous time to discrete time with a sampling time of 10 ms using the c2d command on MATLAB. This is done because the microcontroller in the satellite operates in that manner.

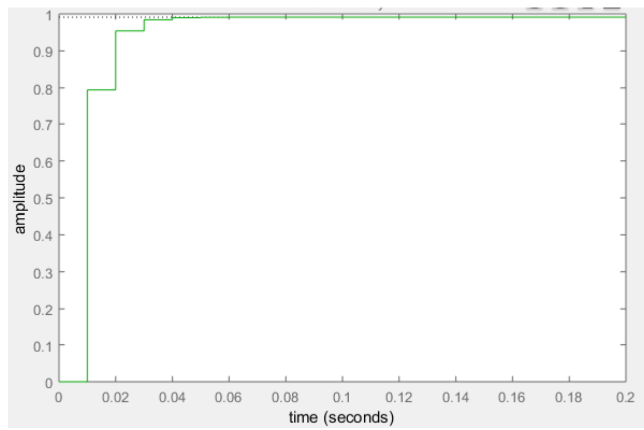

Figure 6. **Step Response Without PID Control**

After the design of the PID controller, the rise time of the close loop transfer function decreases, in this case to 10ms. The equation of the compensator designed is

$$c = 63.288 \times \frac{\left(1 + 0.032z + \left(0.016z\right)^2\right)}{z\left(1 + 0.01z\right)} \tag{20}$$

The step response of the closed loop transfer function has an overshoot and the steady state error of 0.

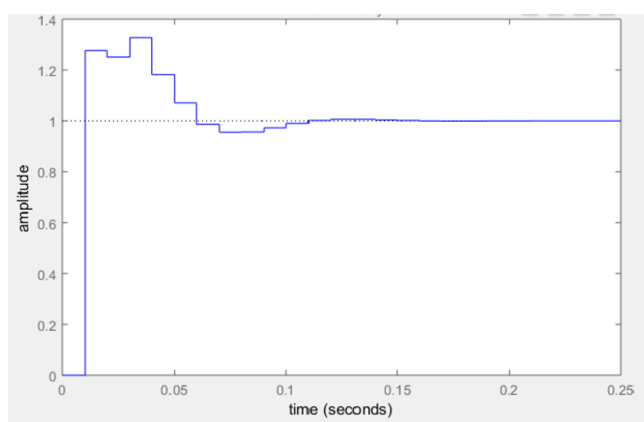

Figure 7. **Step Response With PID Control**

The SVPWM (Space Vector Pulse width modulation) technique is easy to use with microcontrollers as compared to SPWM (Sinusoidal Pulse width modulation). The batteries and the solar cells provide a DC voltage and the BLDC motor operates with a 3 phase AC. SVPWM uses 8 switches to convert this DC to 3 phase AC with minimum harmonics.

7. STRUCTURAL DESIGN OF REACTION WHEEL

The reaction wheel needs to be designed to sustain not only the launch environments, but also the loads encountered during normal operation.

Reaction Wheel Parameters

The design approach of the reaction wheel was to outline the required performance characteristics from the reaction wheel, constraints on the system, and identify critical parameters of the wheel and optimize their values to satisfy the maximum number of requirements.

Parameters to be maximized—

1) Moment of Inertia
2) Outer Diameter
3) Wheel Thickness

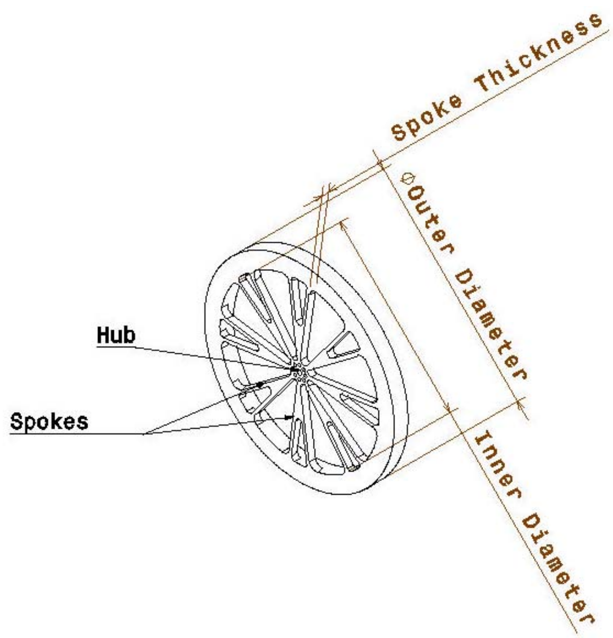

Figure 8. **Wheel Parameters**

Parameters to be minimized—

1) Mass
2) Wheel inner Diameter
3) Number of spokes
4) Spoke thickness
5) Wheel hub thickness

Reaction Wheel Assembly Location

Due to the space constraints in the satellite. There was not any scope for creating a dedicated space to put all the

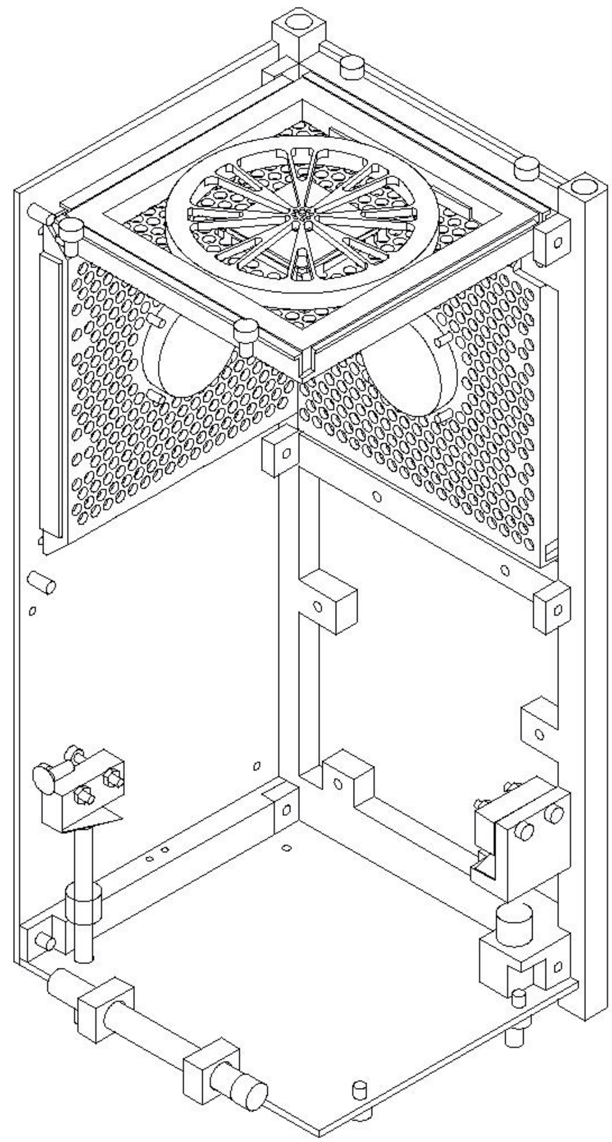

Figure 9. **Placement of Reaction Wheels**

reaction wheels together. Hence it was decided that the reaction wheels would be placed in the space between the three magnetorquers. [Figure 9]

*Wheel outside diameter—*The space available within the magnetorquer limits outside diameter of the reaction wheel. An allowance of 1mm radially was provided on the side closest to the magnetorquer.

*Wheel inside diameter—*The mass constraint limits the inside diameter of the reaction wheel. The mass of the wheel was kept close to 10 grams to accommodate the rest of the assembly and still meet the stringent COG-MOI constraints of the entire satellite.

Wheel Thickness— Increasing the thickness of the reaction wheel increases the moment of inertia of the wheel. However, the height constraints imposed by the pre-existing subassemblies in the satellite limited the thickness of the wheel.

Spoked Design of the Reaction Wheel—Spoked wheels give the highest moment of inertia per unit mass of the wheel. Spoked wheels have the disadvantage of tricky machining and possible wheel balancing issues. However having a solid reaction wheel made the wheel unnecessarily heavy and the moment of inertia obtained for the mass trade-off was unsatisfactory.

Number of spokes—The number of spokes must be minimized to reduce the mass. However having too little spokes compromised the wheels rigidity and stiffness, due to large portions of the wheel rim being unsupported. Hence the number of spokes were finalized as eight. Spoked wheels allowed for a thinner web of the wheel, reducing the mass while simultaneously providing the required strength.

Structural Analysis of Reaction Wheel

The following analyses were performed on the reaction wheel:

1) Static Structural Stresses due to rotation at 6000 rpm

2) Modal - To find the resonant frequencies of the reaction wheel. The resonant frequencies of the wheel should be within the acceptable limits to ensure the vibrations during the launch phase does not induce destructive oscillations in the wheel and its surroundings.

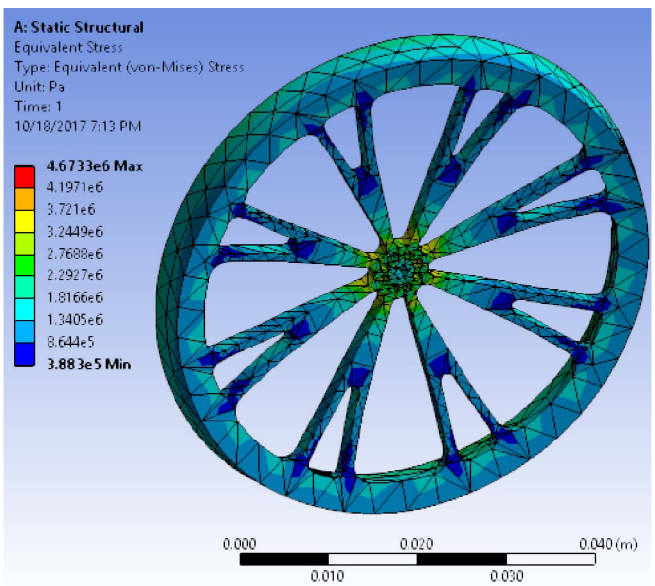

Figure 10. **Static Structural Analysis of the reaction wheel**

Table 2. **Modal Analysis Results**

Mode	Frequency (Hz)
1	725.81
2	777.96
3	778.66
4	1347.7
5	3986.6
6	3988.8

The FEM (Finite Element Method) results show that the working loads are within the safe limits. The maximum stress occurs at the hub during rotation and is equal to 4.6 MPa. It was ensured that the resonant frequencies of reaction wheel did not coincide with that of any other sub-assembly of the satellite or the random vibration loads itself.

8. SUMMARY

In this paper, the complete design of a three-axis attitude control scheme using three reaction wheels is presented. The reaction wheels are coupled with a system of three magnetorquers to dump the momentum which builds up in the reaction wheels over time. All the simulations which are carried over a 2U CubeSat are shown to have satisfactory results as the satellite is able to achieve the desired angular velocities and the targeted pointing location. The electronics design of the reaction wheels is able to achieve the required RPM values by employing a PID controller, thus using a minimum time to achieve the desired speed. The structural design of the reaction wheel system is done by keeping in mind the physical constraints as well as the mass budget. The flywheel design is done in such a manner that the maximum moment of inertia is obtained while keeping the mass of the system to be minimum while not compromising the durability of the system. Hence, the system described in this paper backed by the provided results ensures its suitability for space use.

ACKNOWLEDGMENTS

We would like to take this opportunity to thank Mr. Harish Joglekar, Scientist Engineer at the Indian Space Research Organization (ISRO). This paper could not have been completed without his comprehensive guidance. We also thank Dr. Annadurai M, Chairman SRC, Program Director IRS and SSS at ISRO for providing 'Parikshit' an opportunity to be launched on the Polar Satellite Launch Vehicle (PSLV). We are grateful to Mr. S.A. Kannan, Project Director Small Satellite Systems at ISRO for his support and encouragement shown to Parikshit.

REFERENCES

[1] James R. Wertz, "Attitude Prediction" in Spacecraft Attitude Determination and Control, Boston, Kluwer Academic Publishers, 1990, pp. 558-559

[2] Thomas W. Flatley, Wendy Morgenstern, Alan Reth and Frank Bauer,"B-Dot Acquisition Controller for the RADARSAT Spacecraft", NASA CONFERENCE PUBLICATION, 3345, pp. 79-90, Flight mechanics symposium by NASA,1997.

[3] Raunaq Rakesh, Smit Kamal, Carina Pereira, Naman Saxena, Revathi Ravula, Faraz Haider, Siddhath Mayya and Karun Potty, "Dynamics and Control System Design of a Polar Low-Earth Orbit Nano-Satellite Parikshit", 2015 International Conference on Advances in Computing, Communications and Informatics (ICACCI), August 2015.

[4] M. Chen, S.J. Zhang, F.R. Liu and Y.C. Zhang, "Combined Attitude Control of Small Satellite using One Flywheel and Magnetic Torquers", 2nd International Symposium on Systems and Control in Aerospace and Astronautics (ISSCAA 2008), December 2008.

[5] Vinod KR Singh Patel, A.K.Pandey, "Modeling and Per-

formance Analysis of PID Controlled BLDC Motor and Different Schemes of PWM Controlled BLDC Motor", International Journal of Scientific and Research Publications(IJSRP), Volume 3, Issue 4, April 2013.

BIOGRAPHY

Sai Krishna *is a third year undergraduate student at Manipal Institute of Technology, Manipal, India. He is pursuing a degree in Computer Science and Engineering. He is sub-system head of Attitude Determination and Controls Subsystem of the university funded nano-satellite, "Parikshit". His areas of interest include Artificial Intelligence, Mobile Application Development and Control Systems.*

Sushmita Gosavi *is a second year undergraduate student at Manipal Institute of Technology, Manipal, India. She is pursuing a degree in Information and Communication Technology. She is a part of the ADCS sub-system of University funded nano-satellite, "Parikshit". Her areas of interest include Estimation Algorithms, Software Filters and Control Systems.*

Shivika Singh *is a second year undergraduate student at Manipal Institute of Technology, Manipal, India. She is pursuing a degree in Computer Science and Engineering. She is a part of the ADCS sub-system of University funded nano-satellite, "Parikshit". Her areas of interest include Machine Learning, Orbital Mechanics and Control Systems.*

Naman Saxena *is a Senior year undergraduate student at Manipal Institute of Technology, Manipal, India. He is pursuing a degree in Computer Science and Engineering. He is a member of University funded nano-satellite project Parikshit. His areas of interest include Embedded Systems Software Development, Estimation Algorithms, Control systems, Artificial Intelligence and Cloud Computing.*

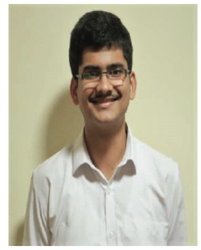

Anirudh Kailaje *is a third year student at Manipal Institute of Technology. He is pursuing his Bachelor's Degree on Mechanical Engineering. He is the Systems Engineer of the university funded nano-satellite, "Parikshit". Finite Element Analysis(FEA) particularly in structural analysis and machine design, CAM and CNC machining are his areas of interest.*

Vishwanath Datla *is a second year undergraduate student at Manipal Institute of Technology, Manipal, India. He is pursuing a degree in Electrical and Electronics Engineering. He is a part of the EPS sub-system of University funded nano-satellite, "Parikshit". His areas of interest include Control Systems and Digital Electronics.*

Paras Shah *is a second year undergraduate student at Manipal Institute of Technology, Manipal, India. He is pursuing a degree in Electronics and Communications Engineering. He is a part of the ADCS sub-system of University funded nano-satellite, "Parikshit".*